International Journal of Environment, Agriculture and Biotechnology
Vol-7, Issue-5; Sep-Oct, 2022

Journal Home Page Available: https://ijeab.com/
Journal DOI: 10.22161/ijeab

Peer Reviewed

Identification of therapeutic potential phytochemicals against the SARS CoV-2 spike protein of omicron variant by Molecular docking techniques

Rathan Kumar

B. E., Department of Biotechnology Engineering, Acharya Institute of Technology, Bengaluru, Karnataka 560 107, India

Received: 01 Oct 2022; Received in revised form: 18 Oct 2022; Accepted: 24 Oct 2022; Available online: 31 Oct 2022

Abstract— *Repeated mutations in the SARS CoV-2 have resulted in the emergence of various life-threatening variants including omicron, triggering a systemic crisis in global human health. Due to the unavailability of any specific antiviral treatment, the effectiveness of the currently available drugs or vaccines against this variant remains doubtful. Phytochemicals from their known medicinal plants were selected with the antiviral, antifungal, anti-inflammatory, and antioxidant properties and screened to study their therapeutic potential and druglikeliness properties. A library* ***of 15*** *phytochemicals from various medicinal plants was constructed and their binding energies were calculated by docking them against the spike protein of the SARS CoV-2 omicron variant using the AutoDock software. Subsequently, the pharmacokinetic properties like ADME and drug likeliness properties were also calculated. Hydroxychloroquine (HCQ), an antimalarial drug was chosen as the standard in docking analysis, displaying the binding energy of -5.22 kcal/mol whereas, Glycyrrhetic acid showed the highest binding energy with the value of -9.02 kcal/mol. Besides, all these 15 phytochemicals showed higher binding energy (≤ -7.00 kcal/mol) with the better pharmacokinetic properties leading them a viable drug candidate to treat the infection caused by omicron variant.*

Keywords— Drug likeliness, Insilico studies, Omicron, Phytochemicals, SARS CoV-2.

I. INTRODUCTION

The emergence and persistence of the coronavirus pandemic that was first identified in Wuhan, China in late December 2019, is still ongoing with a significant rise in the rate of mortality and morbidity.

According to the World Health Organization (WHO) dashboard report, till 28th February 2022, 434,154,739 confirmed cases have been reported globally, including 5,944,342 deaths [1], and an increase in the number of cases has been observed day by day, thus raising the great public health concerns worldwide.

COVID-19 is an infectious disease caused by SARS-CoV-2 (Severe Acute Respiratory Syndrome Coronavirus-2). Genomically, this virus is related to two known CoV-strains, namely the Middle East Respiratory Syndrome Coronavirus (MERS-CoV) emerged in 2012, and the Severe Acute Respiratory Syndrome Coronavirus (SARS-CoV) in late 2003 [2].

The disease is characterized by symptoms such as fever, dry cough, headache, sore throat, fatigue, diarrhoea, and dyspnea followed by acute respiratory distress syndrome [3] and is predominantly known to spread from person-to–person [4]. In addition to this, the virus is also known to infect the upper and lower respiratory tract, liver, kidney, gut, heart, and nervous system and eventually lead to multi-organ damage [5]. Immunocompromised people with obesity, hypertension, diabetes, and cardiovascular disorders are found to be more susceptible[6].

SARS CoV-2 is an enveloped, positive-sense single-stranded RNA virus with a genome size of 26-32 kb [7][8], and is known to be transmitted between animals and

humans [9], belonging to the family Coronaviridae and genus Coronavirus [10].

The viral genome consists of 14 functional open reading frames (ORFs) including two noncoding regions at both ends followed by the multiple regions that encode for 29 proteins including structural, nonstructural proteins (NSP), and accessory proteins. ORF 1a and ORF 1b encode 16 NSPs (nsp1-nsp16) such as Helicase (nsp13), RNA-dependent RNA polymerase (nsp12), Papain-like protease (nsp3), main protease (nsp5) also known as 3C-like protease (3CLpro), and 2O methyltransferase (nsp16), which are likely to be involved in transcription, replication, and pathogenesis and play a vital role in the life cycle of the pathogen. Whereas structural proteins include, Spike surface glycoprotein (S), a small envelope protein (E), membrane protein (M), and nucleocapsid protein (N), which are essential for viral assembly and the production of a structurally whole viral particle. And the remaining 9 are the accessory proteins that provide a selective advantage in the infected host cell [11] [12].

The S protein plays an integral role in viral attachment through the recognition of host cell receptors and promotes the fusion of the viral and host cell membranes, to facilitate the viral entry into the host cells. This protein is composed of two functional subunits: an amino (N)-terminal S1 subunit and a carboxyl (C)-terminal S2 subunit with a single transmembrane region anchor. The S1 subunit consists of an N-terminal domain (NTD) and a receptor-binding domain (RBD), along with two C-terminal domains. Whereas the S2 subunit consists of a fusion peptide (FP), heptad repeat 1 (HR1), central helix (CH) region, connector domain (CD), heptad repeat 2 (HR2), transmembrane (TM) region, and the cytoplasmic tail (CT). The cleavage site at the border between the S1 and S2 subunits is called S1/S2 protease cleavage site [13].

In the native state, the S protein exists as an inactive precursor. During the infection, the S protein gets activated by the TM protease serine 2 (TMPRSS2), a type 2 TM serine protease located on the host cell surface, by cleaving the S protein into S1 and S2 subunits, that are required for activating the membrane fusion domain after the entry of the virus into the host cell [14]. Later, the S1 subunit is shed and the S2 subunit undergoes large conformational change compared to its prefusion state that mediates the membrane fusion process, thus, inserting the fusion peptide into the host cell membrane, followed by the release of viral RNA into the host cell [13], where the polyproteins are translated from the RNA genome. Protein cleavage and the assembly of the replicase–transcriptase complex, make the replication and transcription process of the viral RNA genome occur. The replicated viral RNA and the structural proteins that are newly synthesized are assembled and packaged in the host cell before the release of viral particles [14].

Since, the S protein plays an active role in the recognition, attachment, and fusion of the viral particle into the host cell, thus designing an effective antiviral drug or inhibitor by targeting this protein can be the best solution to treat the infection.

SARS CoV-2 virus, which was previously identified in Wuhan, China in late 2019, has undergone multiple significant mutations resulting in the new variants including Alpha, Beta, Gamma, Delta, Omicron, and so on.

Out of these variants, Omicron is one of the most rapidly spreading SARS CoV-2 variants across the world and has been classified as a “variant of concern (VOC)” by the World Health Organization (WHO) [15].

The first case of the omicron variant (B.1.1.529.1), was reported in South Africa on 23 November 2021 [16] and as of 14 December 2021, it had spread to more than 76 countries [17]. This variant is known to be the highly mutated strain compared to the other VOCs (Alpha, Beta, Gamma, and Delta), with 50 mutations accumulated throughout the genome. Out of which, at least 32 mutations are found in the spike protein, which is twice as many as the Delta variant. These mutations affect the biological characteristics of the omicron variant, by increasing the transmissibility, causing immune escape, and enhancing the virulence. One of the Insilico studies showed that the infectivity of the Omicron variant might be more than 10-fold higher than that of the original virus (Wuhan) [18][19].

The emergence of this variant has posed an increased risk to the global public health, concerning the effectiveness of the currently available drugs or vaccines. At present, most clinical studies are in progress, to study the effect of antiviral drugs, corticosteroids, antimalarials, and monoclonal antibodies against this variant.

Currently, only a few repurposed FDA-approved drugs are being used to treat the infection including Remdesivir, Lopinavir/Ritonavir, Oseltamivir, Favipiravir, Rifampicin, Letermovir, Azithromycin, Cholorquine, and Hydroxychloroquine [20]. Corticosteroids including dexamethasone [21]and methylprednisolone [22], are also being used to treat the infection.

Along with this, scientists worldwide are studying the effectiveness of these drugs alone or with a combination of other antiviral drugs. However, few of the drugs showed certain side effects like cardiotoxicity, hematologic toxicity, hepatotoxicity, and nephrotoxicity.

E.g., Chloroquine and Hydroxychloroquine which were found promising earlier have resulted in neuromyopathy, cardiomyopathy, and retinopathy and was found to decrease in-hospital survival and increased the frequency of ventricular arrhythmias in hospitalized patients [23].

Serum neutralization assay against the omicron variant showed that the neutralization activity of the Pfizer/BNT162b2 mRNA vaccine declined the serum activity by 41.4 fold compared to the original strain (Wuhan) [18][24]. In addition to this, an in vitro study of imdevimab and casirivimab was found to be resistant to authentic omicron variant, which was effectively used to prevent Delta infection [25]. Thus, with the decrease in the vaccine efficacy and unavailability of any specific antiviral drug candidate against the omicron variant, the world is still battling to overcome the Pandemic.

India is home to more than 8000 species of medicinal plants [26]. These plants have been known for their immense potential and tremendous properties against various infectious diseases and health-related complications from ancient times. However, these plants are a rich source of chemically active compounds including alkaloids, flavonoids, terpenoids, polyphenols, tannins, saponins, etc. possessing a variety of biological deliberations, including antioxidant, antibacterial, antifungal, anti-inflammatory, and antiviral properties [27].

At present, plant-based phytochemicals are attracting the focus of modern world healthcare researches, for developing a vaccine or treatment against the infection, since they are known to be less toxic with minimal side effects. It is reported that approximately 70–80% of mainstream medicines originated from natural products [28]. In addition to these, plant-based phytochemicals offer attractive, effective, and holistic drug action against pathogens. Thus, extracting the plant-based compounds and herbal treatments from these plants can be a cure and a solution against omicron infection.

In this regard, Insilico studies were carried out to identify the effect of the phytochemicals that can play a role as an inhibitor by studying their binding affinity towards the spike protein. In the modern world, Insilico studies are gaining much attention worldwide for their advanced strategies and effective techniques for identifying putative drug candidates that can be further led to in vitro and in vivo assessments. These methods basically provide the most accurate results, require shorter time duration, are cost-effective, and fall in the dry lab category, thus being widely used in understanding and predicting the drug ability in the early stages of drug discovery [29].

The current study is aimed to explore the drugs with a therapeutic potential action of the phytochemicals as an effective inhibitor against the spike protein of omicron variant, using Computational pharmacology and virtual screening techniques. A library of 15 phytochemicals was prepared from various medicinal plants, based on their therapeutic potential against infectious diseases. The binding energy of all these phytochemicals was calculated and compared with that of HCQ (an antimalarial drug) which was chosen as the standard reference drug for comparison. Additionally, ADME analysis and drug likeliness studies were also conducted for understanding the safety and efficacy of the phytochemical, which can play a role as the drug candidate for the further development of an effective drug or inhibitor against the infection caused by the omicron variant.

II. MATERIALS & METHODOLOGY

2.1 Preparation of receptor:

The cryo-electron microscopic 3-Dimensional structure of SARS CoV-2 Omicron variant spike protein was downloaded from RCSB-Protein Data Bank with PDB ID: 7T9J [30] and was visualized by using Chimera software 1.14 [31]. In this study, Spike glycoprotein was chosen as the target site. Since, it plays a crucial role in its attachment, fusion, and viral entry into the host cell. The spike protein of the omicron variant consists of 3 chains, Chain A, B, and C as shown in Fig. 1. Out of which, Chain C (represented in Fig. 2) was selected for the docking process, eventually energy minimization and protein optimization was carried out by using the Swiss PDB Viewer [32].

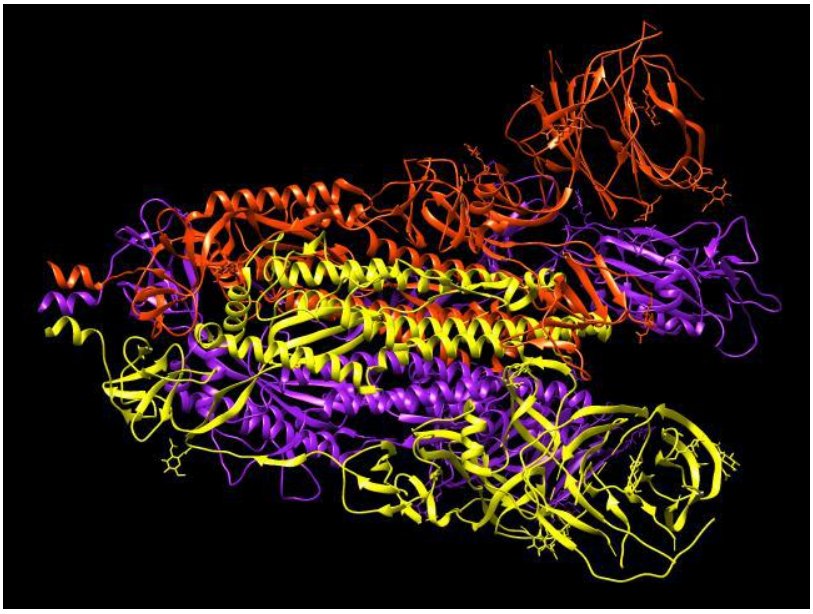

Fig.1: 3D structure of SARS CoV-2 omicron variant spike protein (PDB ID: 7T9J), Chain A (orange-red colored), Chain B (yellow colored), & Chain C (purple colored)

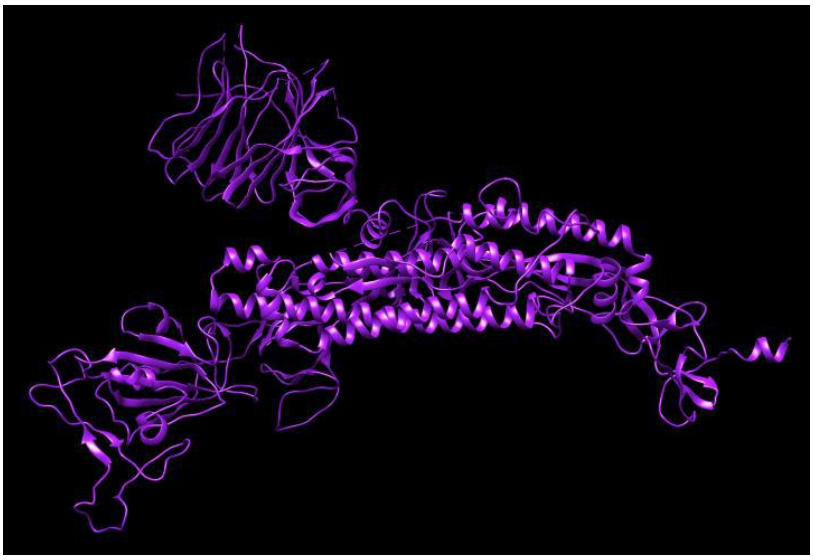

Fig.2: 3D structure of Chain C of SARS CoV-2 omicron variant spike protein

2.2 Protein optimization and energy minimization:

This step is carried out to remove the additional molecules and the extra spaces from the pdb protein files, by arranging the protein coordinates into the proper order. The pdb structure of the protein downloaded from the RCSB-PDB database was opened in WordPad and the individual chain (Chain C) of the protein was retrieved (represented in Fig. 3) and saved in 'all files' format.

```
ATOM  21143  OD1 ASP C1146     190.966 204.982 126.128
1.00114.32           O
ATOM  21144  OD2 ASP C1146     190.670 206.449 127.734
1.00114.32           O
ATOM  21145  N   SER C1147     195.114 205.868 126.562
1.00113.48           N
ATOM  21146  CA  SER C1147     195.814 206.813 125.699
1.00113.48           C
ATOM  21147  C   SER C1147     196.991 206.143 124.998
1.00113.48           C
ATOM  21148  O   SER C1147     197.989 205.797 125.631
1.00113.48           O
ATOM  21149  CB  SER C1147     196.299 208.020 126.505
1.00113.48           C
ATOM  21150  OG  SER C1147     195.229 208.633 127.202
1.00113.48           O
TER   21151      SER C1147
HETATM21152  C1  NAG D   1     173.940 145.791 256.091
1.00189.94           C
HETATM21153  C2  NAG D   1     174.055 145.911 257.627
1.00189.94           C
HETATM21154  C3  NAG D   1     175.262 146.769 258.009
1.00189.94           C
HETATM21155  C4  NAG D   1     176.533 146.234 257.359
```

Fig.3: Protein Optimization using WordPad

Energy minimization of the protein chain was carried out by using the Swiss PDB Viewer tool (v4.1.0), followed by removing the additional swiss coordinates that were added, by using WordPad.

2.3 Ligand preparation:

A library of 15 phytochemicals from numerous medicinal plants was constructed, based on their therapeutic properties. The 3-Dimensional structures of all these phytochemicals including HCQ (PubChem Id: 3652), an antimalarial drug chosen as a standard reference drug were downloaded from the PubChem database in structure-data file (sdf) format. Later, the structure-data file (.sdf) format of these phytochemicals was converted into the pdb format by using Open Babel software 2.4.1 [33] and was visualized in Chimera software 1.14. The pictorial representation of the 3D structure of Glycyrrhetic acid visualized by using Chimera software is represented in figure 4.

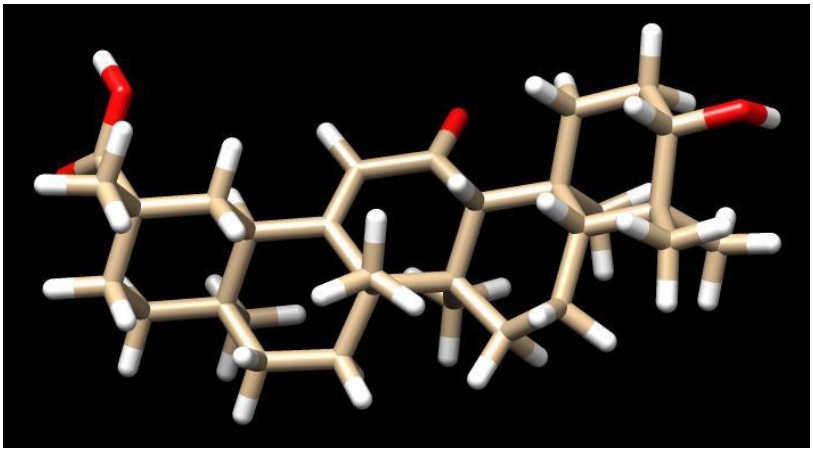

Fig.4: 3D structure of Glycyrrhetic acid.

And Table 1 consists of the name list of all the 15 selected phytochemicals with their PubChem ID's and the scientific name of the medicinal plant from which it is obtained followed by their therapeutic properties.

Table 1: List of phytochemicals isolated from few selected medicinal plants.

Botanical name of the plant	Phytochemical	PubChem Id	Therapeutic properties
Elodea canadensis	β- Sitosterol	222284	Antioxidant [34][35], anti- inflammatory drug [36] and antiviral [37].
Syzygium claviflorum	Betulinic acid	64971	Anti-HIV [38], antimalarial [39], anti-inflammatory, antioxidant and anticancer [40].
Desmodium gangeticum	Desmodin	13338925	Antioxidant [41] and used in the treatment of Alzheimer's disease [42].
Momordica foetida	Foetidin	15945065	Anti-diabetic [43].
Glycyrrhiza glabra	Glycyrrhetic acid	10114	Antiviral [44], immunomodulatory, anti-inflammatory and hepatoprotective [45].
Ferula assa-foetida	Kamolonol	46883037	Antibacterial [46] and cardioprotective property [47].
Marrubium globosum	Marrubiin	73401	Antioxidant, anti- diabetic antinociceptive, antigenotoxic, antioedematogenic, antispasmodic, analgesic, gastroprotective, immunomodulating, cardioprotective and vasorelaxant properties [48].
Salvia tomentosa	Maslinic acid	73659	Anti-inflammatory [49], anticancer [50], anti diabetic [51], antioxidative, cardioprotective [52]and neuroprotective properties [53].
Ophiopogon japonicas	Oleanolic acid	10494	Antioxidative, antiviral, anti-inflammatory, immunomodulatory and cardioprotective properties [45][54].
Prunella vulgaris	Oleanane	9548717	Anticancer, antimicrobial, anti- inflammatory, cytotoxic and hepatoprotective [55].
Gladiolus italicus	Ursolic acid	64945	Antiviral [56], antioxidant, anti-inflammatory and anticancer [45].
Withania somnifera	Withaferin A	265237	Anti platelet, anti herpetic, anti-inflammatory, anticancer, antileishmanial and immunosuppressive properties [57].
Withania somnifera	Withanone	21679027	Antiviral [58], anticancer [59] and neuroprotective [60].
Withania somnifera	Withanolide	53477765	Antiviral [61], anti-inflammatory Immunomodulatory and anti-cancer properties [62].
Plumbago zeylanica	Zeylanone	5276618	Antimicrobial and cytotoxic properties [63]

2.4 Prediction of Active Binding site

An extensive literature survey was conducted to predict the active binding sites on the receptor molecule for docking. Few of the reports suggested that the amino acid residues such as R 493, S 496, and R 498 are considered the active binding amino residues present on the spike protein of the omicron variant [30][64][65].

2.5 Molecular Docking of Receptor and Ligand

The probable inhibitory effects of each of the phytochemicals were evaluated and compared with the std. HCQ by the docking method using AutoDock software 1.5.6 [66]. Prior to the docking process, the protein and the ligands were prepared with the addition of polar hydrogen molecule and Gasteiger charges by removing the water molecules and a few torsion adjustments were made specifically for ligands and were saved in pdbqt format.

The dimension of the grid box was selected as 38Å X 44Å X 56Å with the grid values of X - coordinate = 203.458, Y – coordinate = 181.765 and Z – coordinate = 269.208. The size and dimension of the grid box were selected based on the position of active binding sites of the omicron variant, with a total of 100 genetic runs, while the other parameters were set as default. During the docking process, the receptor (spike protein) was kept rigid and the ligand (phytochemical) was flexible.

The binding affinities of these phytochemicals towards the targeted protein were identified and compared with HCQ. The data generated from the docking process showed how well the ligand gets interacted with the protein of interest. And these values were further analyzed by using MGL tools 1.5.6 [66].

Later, the output files obtained from the docking process were used to study the molecular interactions between the protein-ligand complexes including hydrogen bonds by using Ligplot+ 2.2 software [67].

2.6 ADME analysis & Drug likeliness

The sdf structure of the phytochemical compounds downloaded from the PubChem database was fed into the SwissADME server [68] and converted into canonical SMILES format. These SMILES structures were used to study the ADME (Absorption, Distribution, Metabolism, and Excretion) properties of the screened phytochemicals, and the data obtained from this showed that how well a chemical drug (phytochemical) is processed in a living organism.

Some of the important parameters related to the drug likeness properties of the compounds including molecular weight, number of hydrogen bond donors, number of hydrogen bond acceptors, and molar refractivity were computed utilizing Lipinski's rule of five [69].

III. RESULTS

The current study was focused on identifying the specific antiviral drug or inhibitor by targeting the spike glycoprotein of the omicron variant by drug repurposing technique since this protein plays a prime role in its attachment and internalization into the host cells. Thus, identifying a new drug or inhibitor which can inhibit the binding of the spike glycoprotein to the host cell can be a solution against the infection.

3.1 Virtual Screening and Visualization

Molecular docking is the most promising tool in the drug discovery process, which is used to predict the binding affinity of the ligand towards the targeted protein molecule when the 3D structure of the target protein is known. It is also used to study the interactions between the protein-ligand complexes at the atomic level and characterize the behavior of ligands in the binding site of target proteins as well as elucidate fundamental biochemical processes [70]. Because of their wide applications, this method is mostly preferred in all pharmaceutical industries. Hence, this method was employed to study the therapeutic potential of the selected phytochemicals including HCQ against the SARS CoV-2 omicron variant based on their binding affinity of the phytochemical (ligand) towards the targeted protein (spike protein).

Higher the negative value of the binding energy stronger the binding of the phytochemical towards the targeted protein.

The binding energy of all the 15 phytochemicals against the spike protein of the SARS CoV-2 omicron variant was calculated by AutoDock software 1.5.6. The 2D structure of the selected phytochemicals along with their binding energies and interacting residues are represented in Table 2.

Table 2: The binding energy of the compound towards the spike protein of the omicron variant along with their interacting residues with the grid dimension of 38 X 44 X 56 (Å) and grid value of X = 203.458, Y = 181.765 and Z = 269.208 (The 2D structure of all the ligands represented in the above table are downloaded from PubChem database)

Name of the ligand	**2D-Structure**	**Binding energy (kcal/mol)**	**Interacting amino acid residues**
Hydroxychloroquine	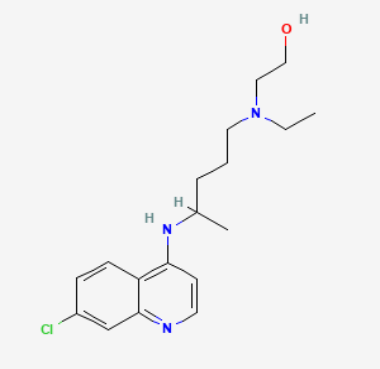	-5.22	Hydrogen bond (H- bond): ARG 403, ARG 493, ARG 498 and HIS 505. Hydrophobic interactions (H-I): TYR 449, TYR 453, SER 494, TYR 495, SER 496, PHE 497 and TYR 501.
β- Sitosterol	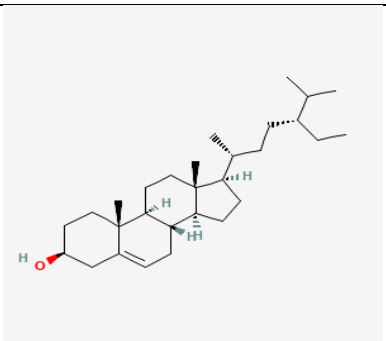	-7.45	H- bond: HIS 505. H-I: ARG 403, TYR 453, ARG 493, SER 494, TYR 495, SER 496, PHE 497 and TYR 501.
Betulinic acid	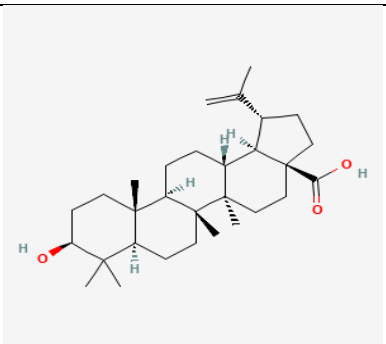	-7.46	H- bond: ARG 493. H-I: ARG 403, TYR 453, SER 494, TYR 495, SER 496, PHE 497 and HIS 505.
Desmodin	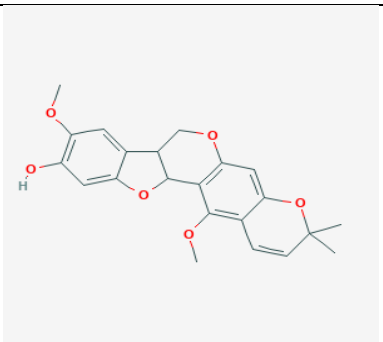	-7.07	H- bond: SER 494. H-I: ARG 403, TYR 449, TYR 453, ARG 493, TYR 495, SER 496, PHE 497 and HIS 505.

Foetidin	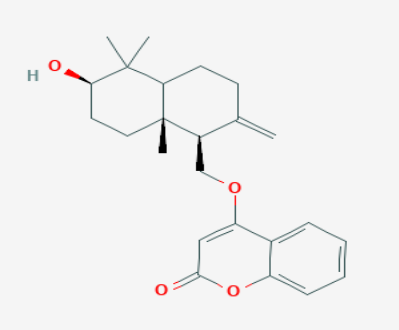	-7.36	H- bond: ARG 493. H-I: ARG 403, TYR 449, TYR 453, SER 494, TYR 495, SER 496, PHE 497, TYR 501 and HIS 505.
Glycyrrhetic acid	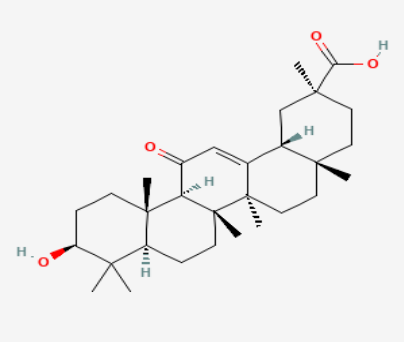	-9.02	H- bond: TYR 453 and SER 494. H-I: ARG 403, ARG 493, TYR 495, SER 496, TYR 501 and HIS 505.
Kamolonol	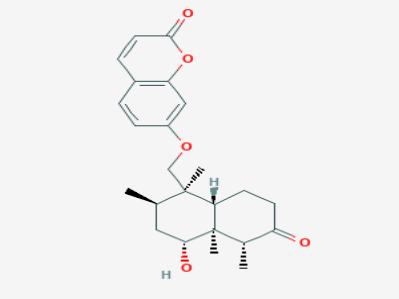	-7.41	H- bond: TYR 453 and SER 494. H-I: ARG 403, ARG 493, TYR 495, SER 496, PHE 497, TYR 501 and HIS 505.
Marrubiin	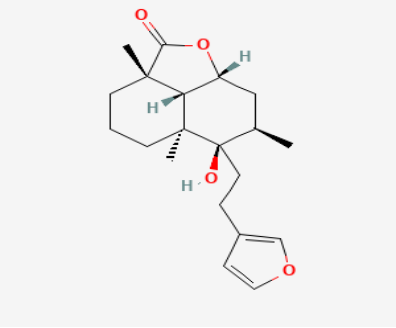	-7.09	H- bond: SER 496. H-I: ARG 403, TYR 453, SER 494, TYR 495, PHE 497, TYR 501 and HIS 505.
Maslinic acid	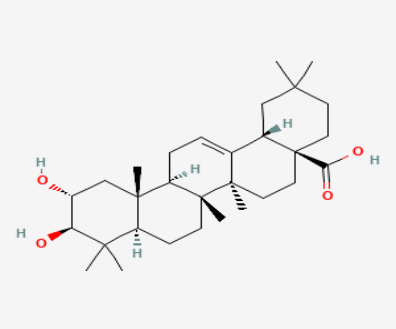	-8.17	H- bond: ARG 493. H-I: ARG 403, TYR 453, SER 494, TYR 495, SER 496, PHE 497, TYR 501 and HIS 505.

Oleanolic acid	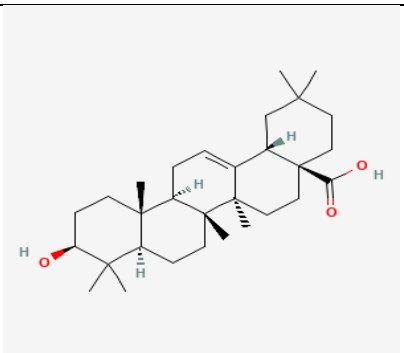	-8.68	H- bond: ARG 493. H-I: ARG 403, TYR 453, SER 494, TYR 495, SER 496, TYR 501 and HIS 505.
Oleanane	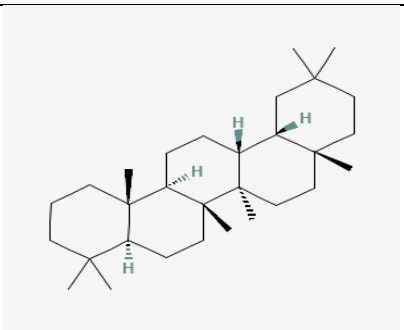	-7.63	H-I: ARG 403, ARG 493, SER 494, TYR 495, SER 496, PHE 497, TYR 501 and HIS 505.
Ursolic acid	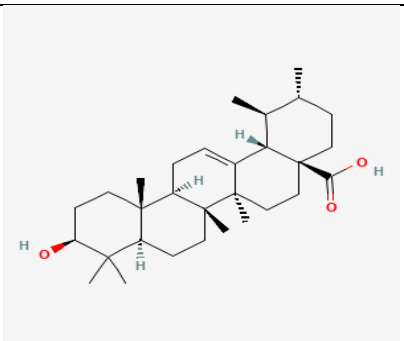	-8.54	H- bond: ARG 493. H-I: ARG 403, TYR 453, SER 494, TYR 495, SER 496, PHE 497, TYR 501 and HIS 505.
Withaferin A	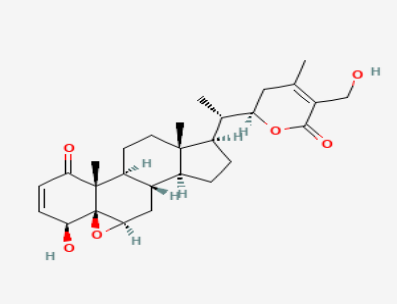	-7.53	H- bond: TYR 449 and SER 496. H-I: ARG 403, TYR 453, ARG 493, SER 494, TYR 495, PHE 497, TYR 501 and HIS 505.
Withanone	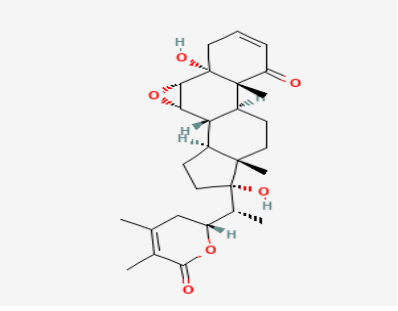	-8.12	H- bond: ARG 403, SER 494 and SER 496. H-I: TYR 449, TYR 453, ARG 493, TYR 495, PHE 497 and HIS 505.

Withanolide	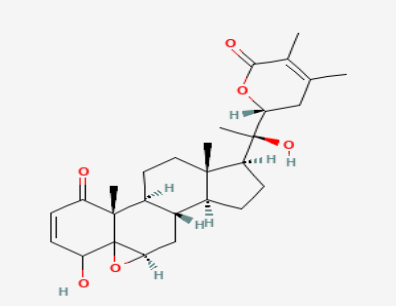	-7.73	H- bond: SER 494 and SER 496. H-I: ARG 403, TYR 453, ARG 493, TYR 495, PHE 497, TYR 501 and HIS 505.
Zeylanone	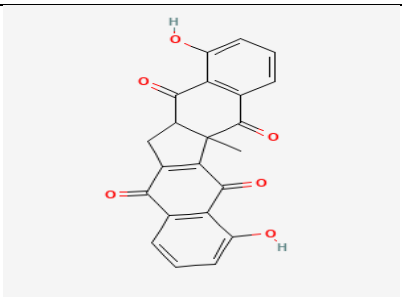	-7.21	H- bond: ARG 493 and SER 496. H-I: TYR 453, SER 494, TYR 495, PHE 497, TYR 501 and HIS 505.

From Table 2, we can observe that the binding energy of all the 15 selected phytochemicals was higher (≤ -7.00 kcal/mol) than the HCQ which was chosen as the std. reference drug to study and compare the binding affinity of these phytochemicals against the spike protein.

The binding energy of standard drug HCQ was found to be -5.22 kcal/mol whereas, Glycyrrhetic acid showed the highest binding energy among all 15 phytochemicals with the value of -9.02 kcal/mol towards the active site of the target protein, followed by Oleanolic acid with the value of -8.68 kcal/mol, Ursolic acid -8.54, Maslinic acid -8.17, Withanone -8.12, Withanolide -7.73, Oleanane -7.63, Withaferin A -7.53, Betulinic acid -7.46, β- sitosterol -7.45, Kamolonol -7.41, Foetidin -7.36, Zeylanone -7.21, Marrubiin -7.09 and Desmodin which showed the lowest binding energy of value -7.07 kcal/mol. The binding of the receptor protein (7T9J_C) with each ligand (phytochemical) is represented in Figure 5(a)-20(a). Protein-ligand interactions of each phytochemical were estimated by Ligplot+ 2.2 software and are represented in Figure 5(b)-20(b).

ARG 403, ARG 493, ARG 498 and HIS 505 were the four amino acid residues involved in the hydrogen bond with HCQ. TYR 449, TYR 453, SER 494, TYR 495, SER 496, PHE 497 and TYR 501 were the amino acids involved in hydrophobic interactions with the spike protein. Glycyrrhetic acid formed hydrogen bonds with the TYR 453 and SER 494. ARG 403, ARG 493, TYR 495, SER 496, TYR 501 and HIS 505 were the amino acid residues of spike protein that interacted with Glycyrrhetic acid by hydrophobic interaction. Similarly, Oleanolic acid showed the hydrogen interaction with the ARG 493 whereas, ARG 403, TYR 453, SER 494, TYR 495, SER 496, TYR 501 and HIS 505 showed the hydrophobic interaction with the amino acid residues of the spike protein. ARG 493 amino acid residue of spike protein was involved in hydrogen bonding with the Ursolic acid. Besides, ARG 403, TYR 453, SER 494, TYR 495, SER 496, PHE 497, TYR 501 and HIS 505 were involved in hydrophobic interaction with the targeted site of the protein. Maslinic acid formed a hydrogen bond with the ARG 493. In addition to this, ARG 403, TYR 453, SER 494, TYR 495, SER 496, PHE 497, TYR 501 and HIS 505 were the amino acids involved in hydrophobic interactions with the spike protein. Withanone showed hydrogen bonding with ARG 403, SER 494 and SER 496 amino acid residues and moreover interacted with TYR 449, TYR 453, ARG 493, TYR 495, PHE 497 and HIS 505 amino acids residues by hydrophobic interactions. Withanolide formed hydrogen bonds with the SER 494 and SER 496 residues. ARG 403, TYR 453, ARG 493, TYR 495, PHE 497, TYR 501 and HIS 505 amino acid residues of spike protein interacted with Withanolide by hydrophobic interaction. Oleanane showed the hydrophobic interaction with the ARG 403, ARG 493, SER 494, TYR 495, SER 496, PHE 497, TYR 501 and HIS 505 amino acid residues of the spike protein, whereas it didn't show hydrogen interaction with the any of the amino acid residues of the spike protein. Withaferin A showed hydrogen bonding with TYR 449 and SER 496. Moreover, it interacted with ARG 403, TYR 453, ARG 493, SER 494, TYR 495, PHE 497, TYR 501 and HIS 505 amino acid residues via hydrophobic interaction. The Betulinic acid formed a hydrogen bond with the ARG 493. ARG 403, TYR 453, SER 494, TYR 495, SER 496, PHE 497 and HIS 505 showed the hydrophobic interaction with the amino acid residues of the spike protein.

Similarly, β-sitosterol showed the H- bond with HIS 505, whereas, hydrophobic interactions with the ARG 403, TYR 453, ARG 493, SER 494, TYR 495, SER 496, PHE 497 and TYR 501 amino acid residues with the targeted protein site. TYR 453 and SER 494 residues of spike protein were involved in H-bond formation with Kamolonol. Besides, ARG 403, ARG 493, TYR 495, SER 496, PHE 497, TYR 501 and HIS 505 residues showed the hydrophobic interactions with the spike protein. Foetidin formed H-bond with ARG 493 amino acid residue. Moreover, Foetidin interacted with the ARG 403, TYR 449, TYR 453, SER 494, TYR 495, SER 496, PHE 497, TYR 501 and HIS 505 residues hydrophobically. Zeylanone showed hydrogen bonding with ARG 493 and SER 496. In addition to this, Zeylanone interacted with TYR 453, SER 494, TYR 495, PHE 497, TYR 501 and HIS 505 amino acid residues via hydrophobic interaction. Similarly, Marrubiin formed a hydrogen bond with the SER 496 amino acid residue. Furthermore, it interacted with the ARG 403, TYR 453, SER 494, TYR 495, PHE 497, TYR 501 and HIS 505 residues hydrophobically. The Desmodin formed a hydrogen bond with the SER 494 amino acid residue. In addition to this, Desmodin interacted with the ARG 403, TYR 449, TYR 453, ARG 493, TYR 495, SER 496, PHE 497 and HIS 505 residues hydrophobically.

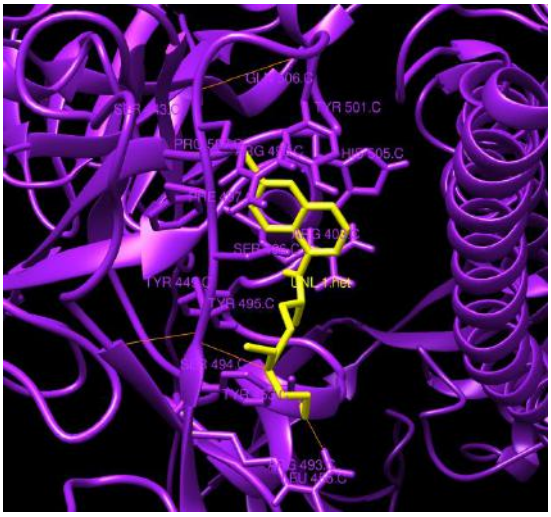

Fig.5(a): 7T9J_C - HCQ

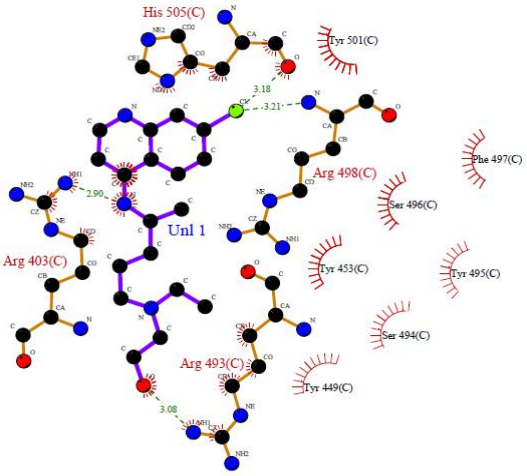

Fig.5(b): 7T9J_C - HCQ

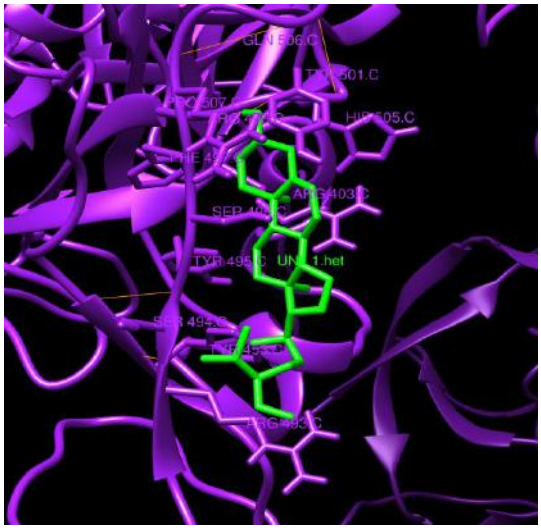

Fig. 6(a): 7T9J_C - β- Sitosterol

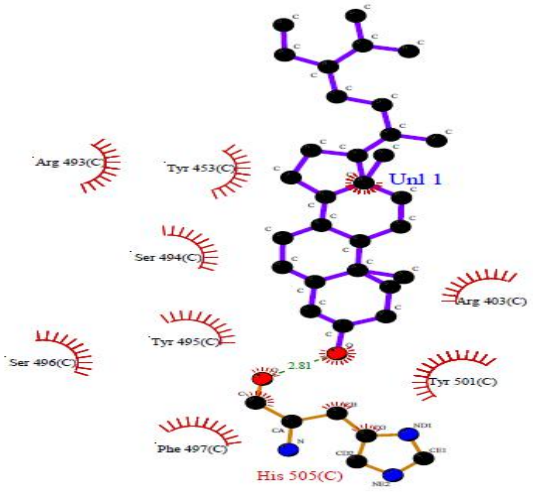

Fig. 6(b): 7T9J_C - β- Sitosterol

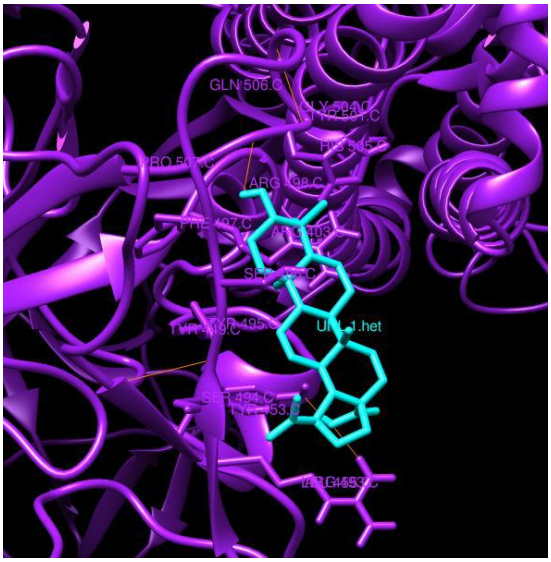

Fig. 7(a): 7T9J_C - Betulinic acid

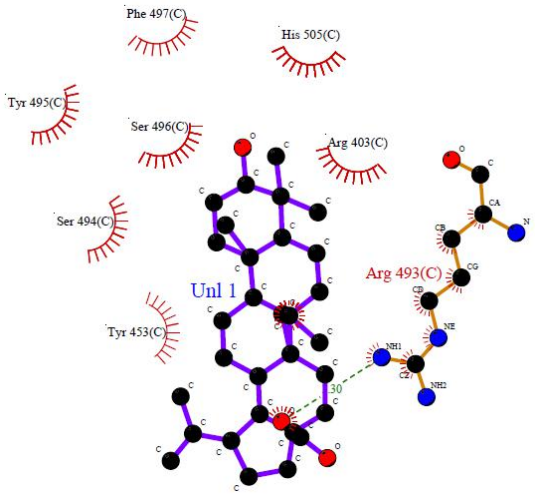

Fig. 7(b): 7T9J_C - Betulinic acid

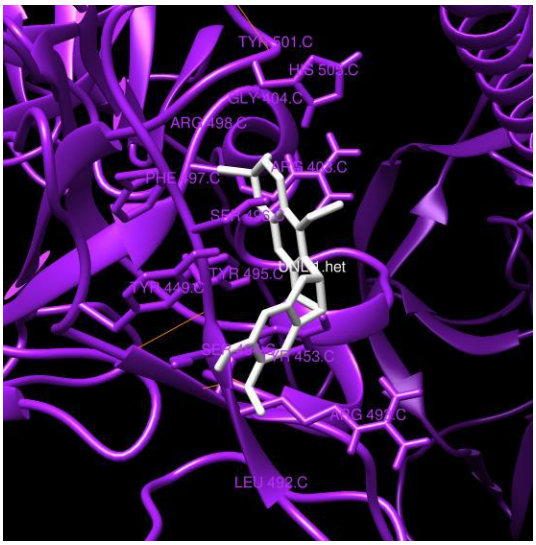

Fig. 8(a): 7T9J_C - Desmodin

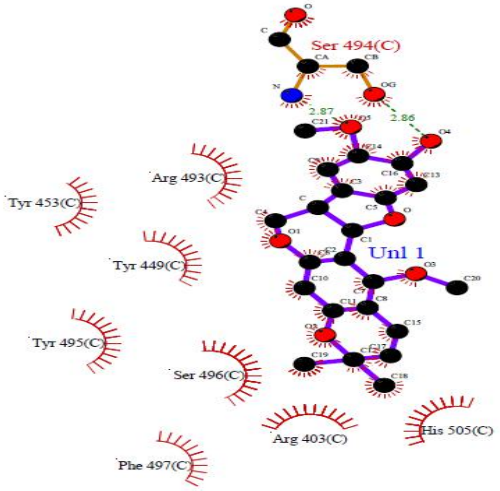

Fig. 8(b): 7T9J_C - Desmodin

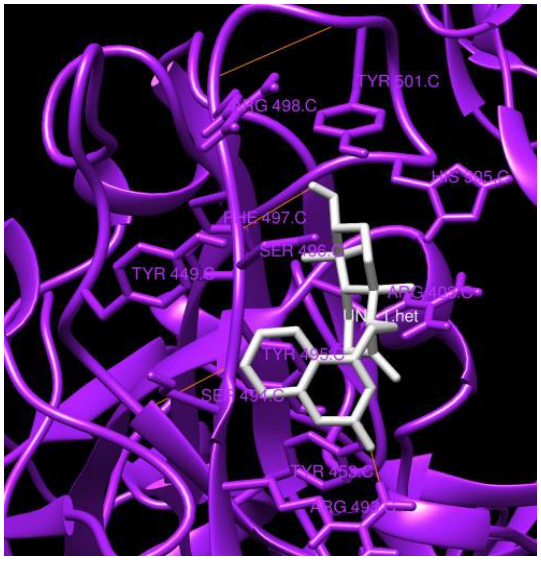

Fig. 9(a): 7T9J_C – Foetidin

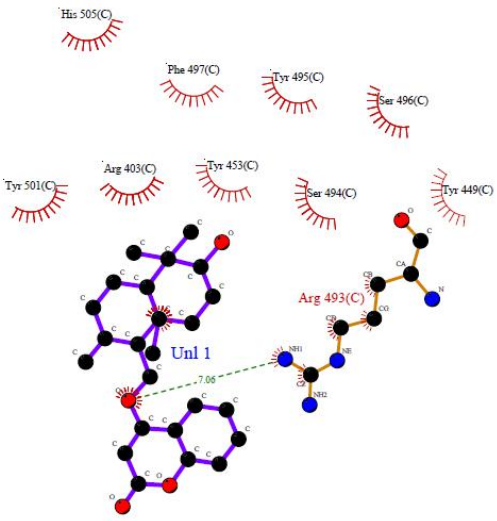

Fig. 9(b): 7T9J_C - Foetidin

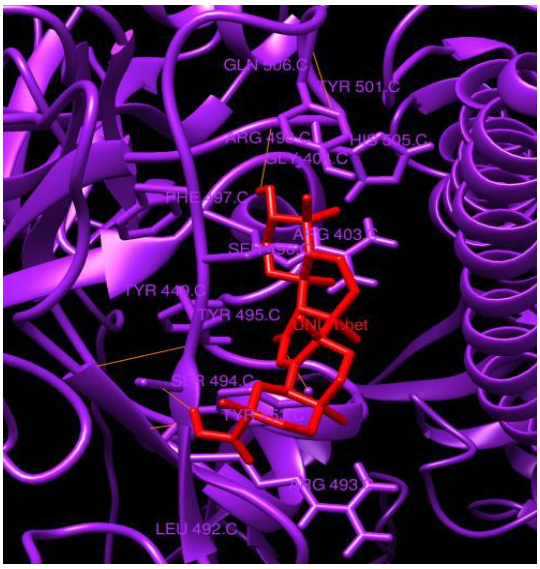

Fig. 10(a): 7T9J_C - Glycyrrhetic acid

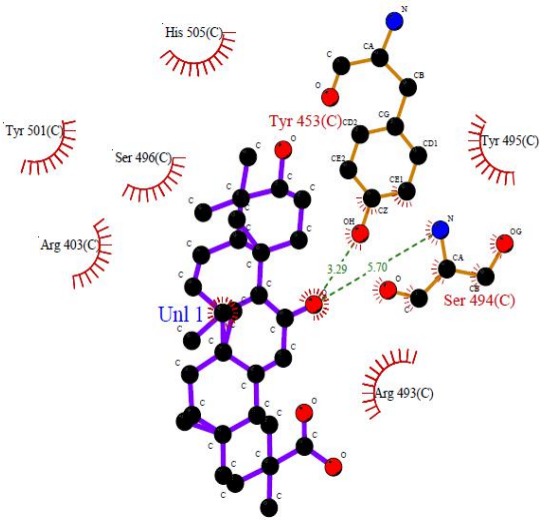

Fig. 10(b): 7T9J_C - Glycyrrhetic acid

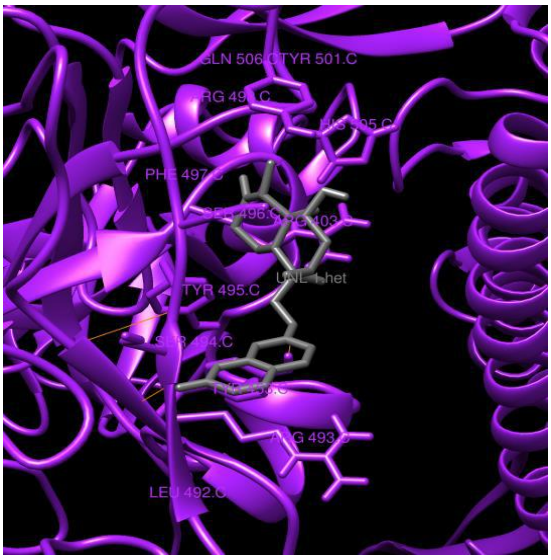

Fig. 11(a): 7T9J_C - Kamolonol

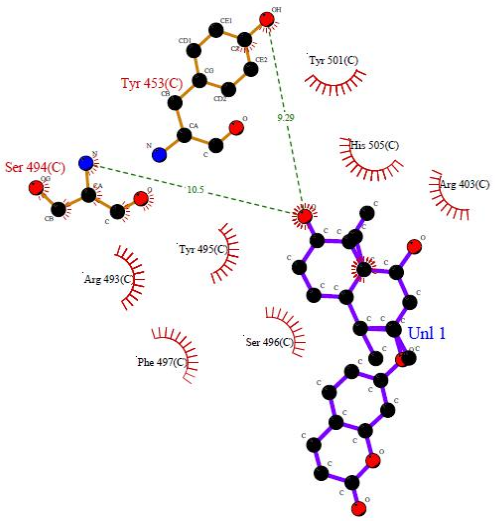

Fig. 11(b): 7T9J_C - Kamolonol

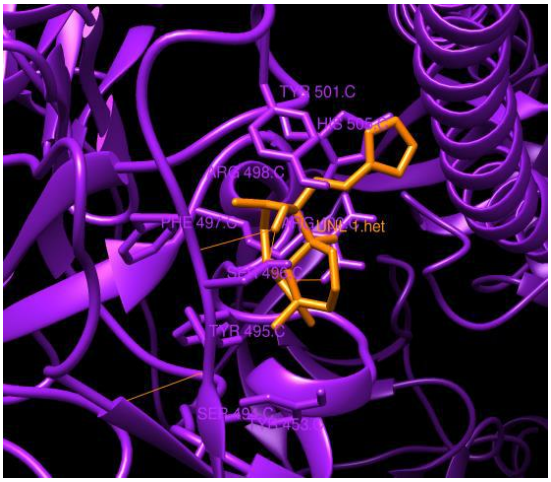

Fig. 12(a): 7T9J_C - Marrubiin

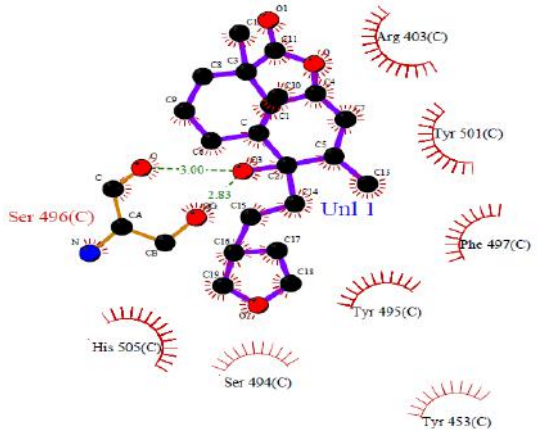

Fig. 12(b): 7T9J_C - Marrubiin

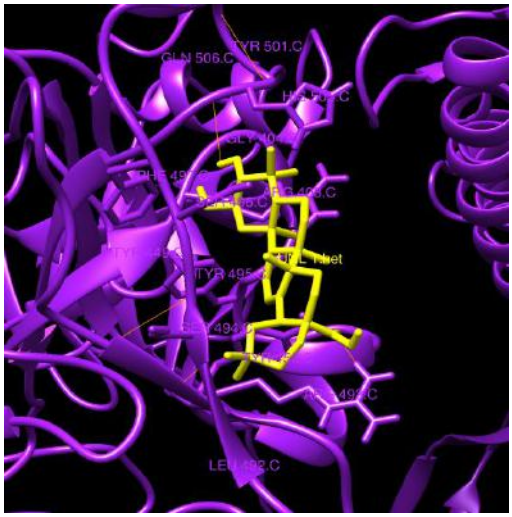

Fig. 13(a): 7T9J_C - Maslinic acid

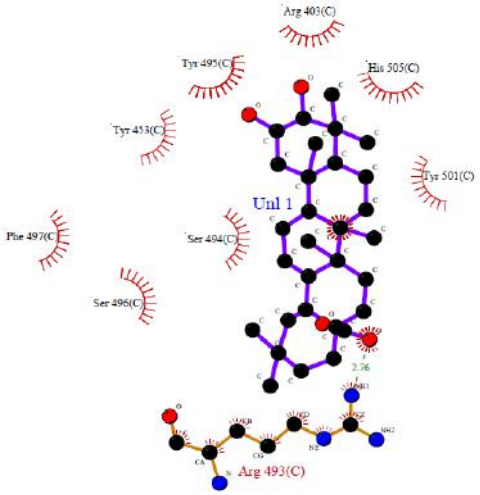

Fig. 13(b): 7T9J_C - Maslinic acid

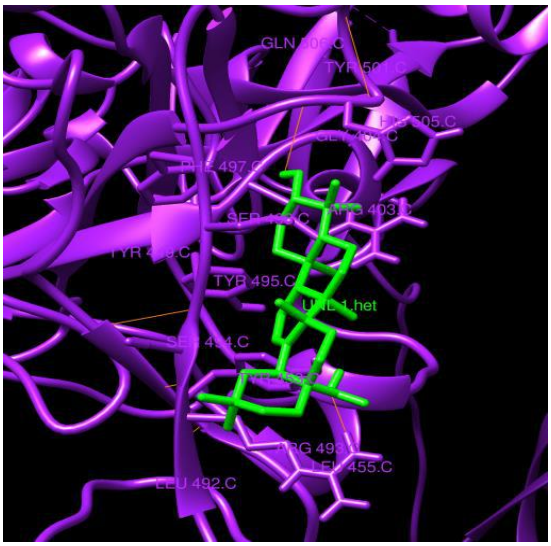

Fig. 14(a): 7T9J_C - Oleanolic acid

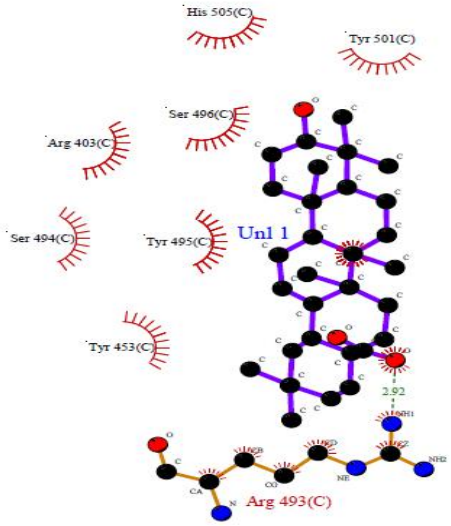

Fig. 14(b): 7T9J_C - Oleanolic acid

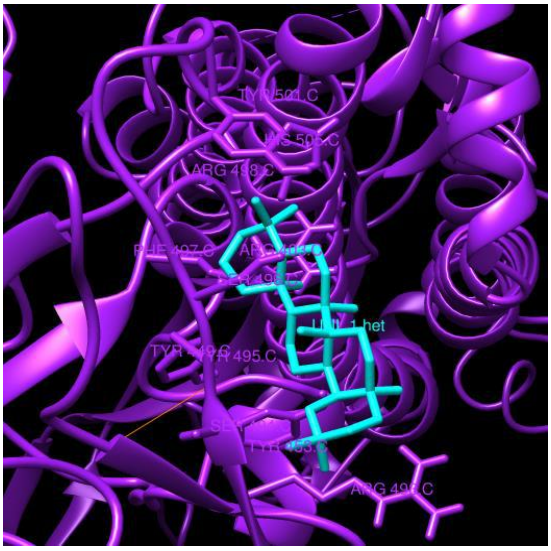

Fig. 15(a): 7T9J_C – Oleanane

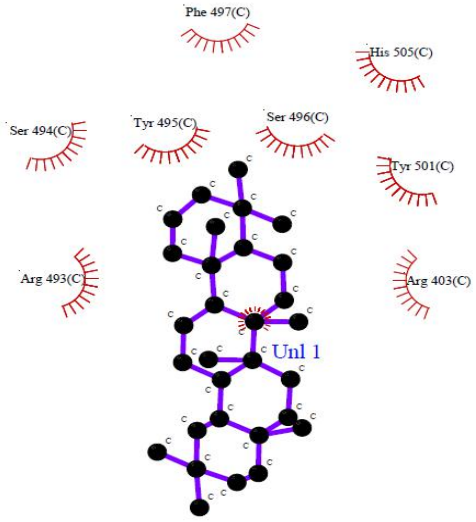

Fig. 15(b): 7T9J_C – Oleanane

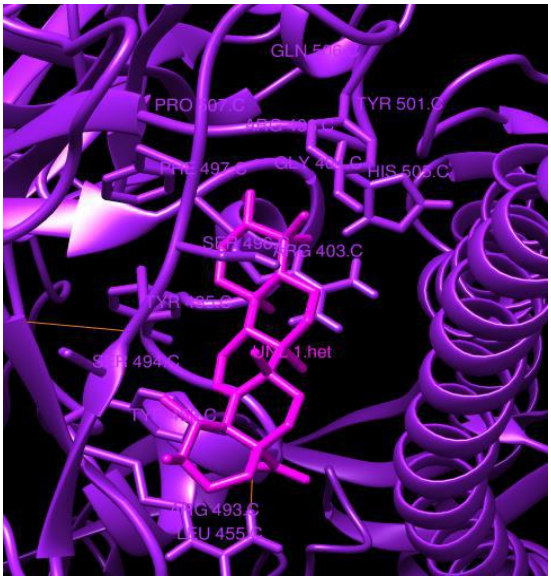

Fig. 16(a): 7T9J_C – Ursolic acid

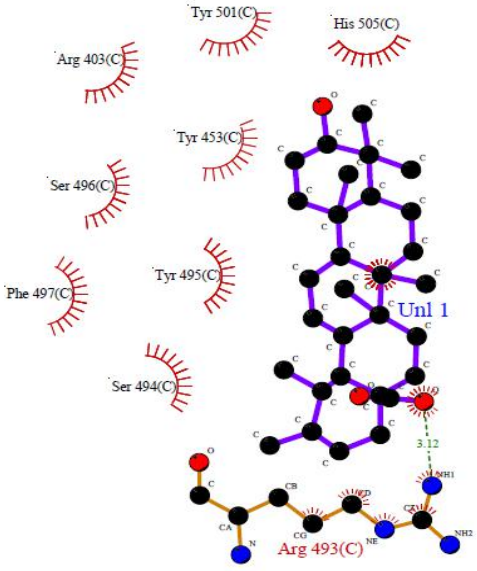

Fig. 16(b): 7T9J_C – Ursolic acid

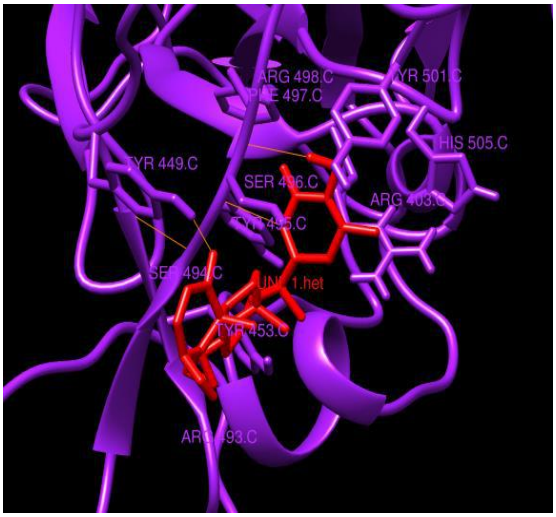

Fig. 17(a): 7T9J_C – Withaferin A

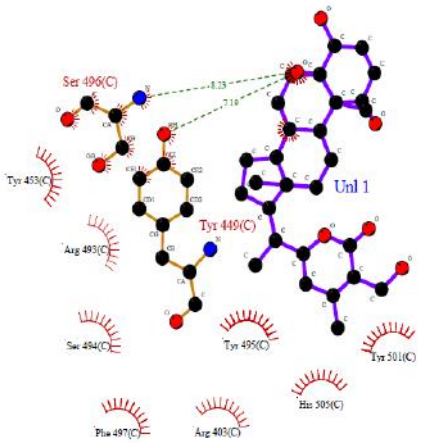

Fig. 17(b): 7T9J_C – Withaferin A

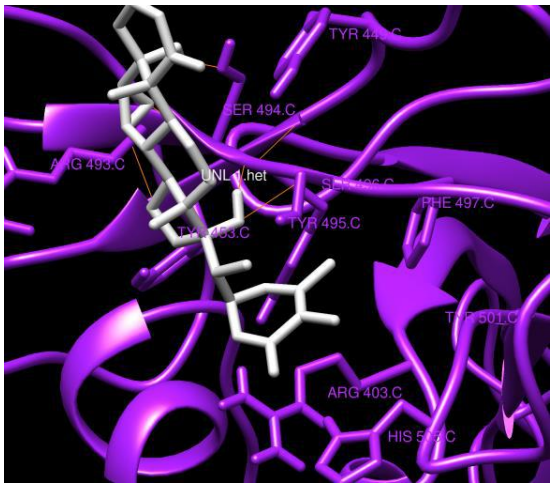

Fig. 18(a): 7T9J_C – Withanone

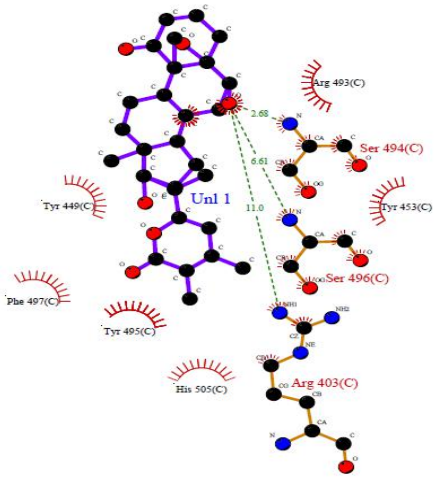

Fig. 18(b): 7T9J_C – Withanone

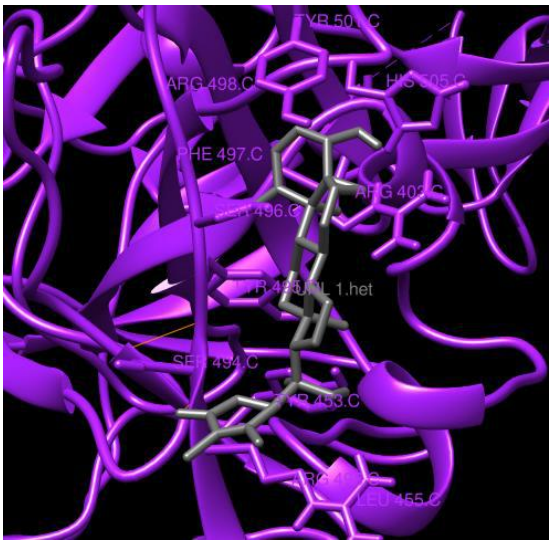

Fig. 19(a): 7T9J_C – Withanolide

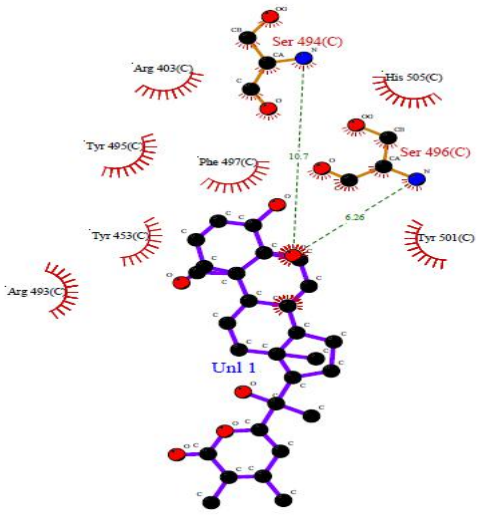

Fig. 19(b): 7T9J_C – Withanolide

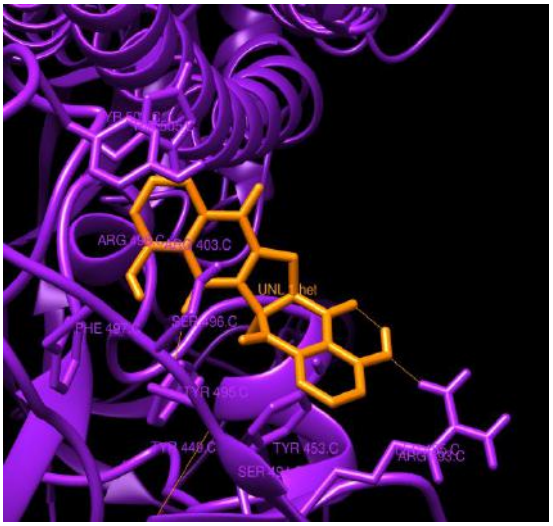

Fig. 20(a): 7T9J_C – Zeylanone

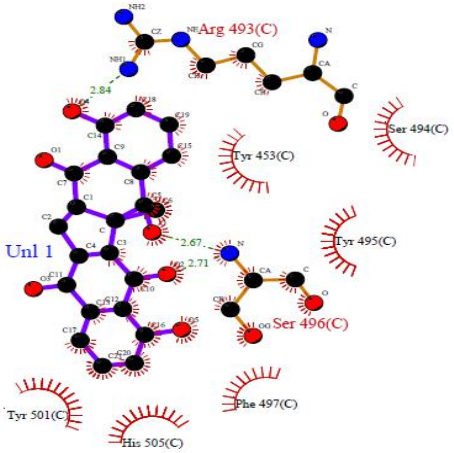

Fig. 20(b): 7T9J_C – Zeylanone

Fig.5(a)-20(a): Crystal structure of the protein receptor-binding domains (7T9J_C) and ligand complexes of HCQ, β-Sitosterol, Betulinic acid, Desmodin, Foetidin, Glycyrrhetic acid, Kamolonol, Marrubiin, Maslinic acid, Oleanolic acid, Oleanane, Ursolic acid, Withaferin A, Withanone, Withanolide, and Zeylanone.

Fig.5(b)-20(b): Hydrogen and hydrophobic interactions of all the compounds with the spike protein of the omicron variant (7T9J_C).

3.2 ADME studies & Drug likeliness prediction

Besides, the calculating the binding energy and the molecular interactions between the protein and the ligand, compounds were further allowed for ADME analysis. These properties evaluate the ability of a compound to act as a drug, which follows Lipinski's Rule of Five.

Lipinski's rule of five is a rule of thumb that describes the drug likeliness of a compound, with specific therapeutic properties that are likely to have chemical and physical properties that would make it an orally active drug. This rule figures out a few of the molecular properties that are essential for the drug pharmacokinetics in the human body, such as Absorption, distribution, metabolism, and excretion.

Lipinski's rule of five states that the chemical compound must follow the below-mentioned criteria to be considered a safe drug,

1. Molecular mass > 500 Da
2. A logarithm octanol-water partition coefficient (MlogP) > 4.15

3. Number of H-bond donors > 5
4. Number of H-bond acceptors >10

The violation of 2 or more conditions anticipates that the compound is not orally active [71]. Swiss ADME web server was used to study the ADME properties of the phytochemicals. Table 3 shows the ADME analysis data obtained from the SwissADME server for all the 15 phytochemicals along with HCQ.

Table 3: ADME properties of the few selected compounds

Name of the Phytochemical	Molecular Weight (<500 Da)	MlogP (<4.15)	H – Bond Acceptor (<10)	H – Bond Donor (<5)	Violations	Drug Likeliness
Hydroxychloroquine	335.87	2.35	3	2	0	Yes
β- Sitosterol	414.71	6.73	1	1	1	Yes
Betulinic acid	456.70	5.82	3	2	1	Yes
Desmodin	382.41	2.06	6	1	0	Yes
Foetidin	382.49	3.83	4	1	0	Yes
Glycyrrhetic acid	470.68	4.87	4	2	1	Yes
Kamolonol	398.49	3.00	5	1	0	Yes
Marrubiin	332.43	2.76	4	1	0	Yes
Maslinic acid	472.70	4.97	4	3	1	Yes
Oleanolic acid	456.7	5.82	3	2	1	Yes
Oleanane	412.73	9.05	0	0	1	Yes
Ursolic acid	456.70	5.82	3	2	1	Yes
Withaferin A	470.6	2.75	6	2	0	Yes
Withanone	470.6	2.75	6	2	0	Yes
Withanolide	470.6	2.75	6	2	0	Yes
Zeylanone	374.34	0.69	6	2	0	Yes

From Table 3, we can observe that all the 15 phytochemicals followed the Lipinski rule of five. Out of which, 8 phytochemicals including Desmodin, Foetidin, Kamolonol, Marrubiin, Withaferin A, Withanone, Withanolide, and Zeylanone showed no violations. And the remaining 7 phytochemicals including β- Sitosterol, Betulinic acid, Glycyrrhetic acid, Maslinic acid, Oleanolic acid, Oleanane, and Ursolic acid showed one violation (MlogP < 4.15) in Lipinski rule of five.

The data obtained from Table 3, shows that all the selected phytochemicals followed the Lipinski rule of five with not more than 1 violation, making them a suitable drug candidate for the treatment against the omicron variant.

The current study was focused on identifying the inhibitory potential of the 15 selected phytochemicals by targeting the active sites of SARS CoV-2 omicron variant spike protein. This protein was chosen as the druggable target site, since it plays a crucial role in the recognition, attachment, and fusion of the virus into the host cell. There are several chemotherapeutic drugs such as Remdesivir, Azithromycin, Amantadine, and many more that are being used to treat the infection. But, few of the drugs showed certain side effects like low blood pressure, vomiting, nausea, orthostatic hypotension, allergic reactions, and others. In addition to this, higher uptake of chemotherapeutic drugs might cause severe toxic effects on the human body that can lead to organ dysfunction.

Hence, there is an urgent need for developing an effective drug or inhibitor against the omicron variant with the least toxic effects. As a consequence of that, these phytochemicals can be the best solution for the treatment, whose binding energies were found to be 1.5-1.8 times higher than the std. HCQ, following the Lipinski rule of

five criteria and are known to be safer with no or fewer side effects, thus intimating that these phytochemicals have the potential to form an antiviral drug or inhibitor against the SARS CoV-2 omicron variant.

IV. CONCLUSION

The mutating nature of the SARS CoV-2 has resulted in the emergence of omicron; another new variant with a higher fatality rate has created urgency for the development of new antiviral drugs or vaccines against the infection. In this regard, the research study was carried out, to identify the therapeutic potential of the phytochemicals from different medicinal plants against the spike protein of the omicron variant using Insilico approaches. This study showed that the binding energy of all the 15 phytochemicals was higher compared to the std. HCQ with the greater potential of inhibiting the binding of the viral spike protein to the host cell receptor. In addition to this, the phytochemicals also fulfilled all the criteria of the drug likeliness and ADME studies. Therefore, the results obtained from the current study suggest that all these 15 phytochemicals can be used as lead molecules for designing an effective drug against the omicron variant.

However, the data obtained from the current study is based on the Insilico approach, additional studies have to be carried out with in vitro and in vivo conditions using animal models to check the feasibility of the compound.

REFERENCES

[1] WHO, "Weekly Operational Update on COVID-19," *Emerg. Situational Updat.*, no. 77, pp. 1–10, 2022.

[2] E. De Wit, N. Van Doremalen, D. Falzarano, and V. J. Munster, "SARS and MERS: Recent insights into emerging coronaviruses," *Nat. Rev. Microbiol.*, vol. 14, no. 8, pp. 523–534, 2016, doi: 10.1038/nrmicro.2016.81.

[3] M. Abdalla *et al.*, "In silico studies on phytochemicals to combat the emerging COVID-19 infection," *J. Saudi Chem. Soc.*, vol. 25, no. 12, p. 101367, 2021, doi: 10.1016/j.jscs.2021.101367.

[4] I. Ghinai *et al.*, "First known person-to-person transmission of severe acute respiratory syndrome coronavirus 2 (SARS-CoV-2) in the USA," *Lancet*, vol. 395, no. 10230, pp. 1137–1144, 2020, doi: 10.1016/S0140-6736(20)30607-3.

[5] A. Kumar, D. C. Mishra, U. B. Angadi, R. Yadav, A. Rai, and D. Kumar, "Inhibition Potencies of Phytochemicals Derived from Sesame Against SARS-CoV-2 Main Protease: A Molecular Docking and Simulation Study," *Front. Chem.*, vol. 9, no. October, pp. 1–16, 2021, doi: 10.3389/fchem.2021.744376.

[6] S. H. de C. Sales-Peres, L. J. de Azevedo-Silva, R. C. S. Bonato, M. de C. Sales-Peres, A. C. da S. Pinto, and J. F. Santiago Junior, "Coronavirus (SARS-CoV-2) and the risk of obesity for critically illness and ICU admitted: Meta-analysis of the epidemiological evidence," *Obes. Res. Clin. Pract.*, vol. 14, no. 5, pp. 389–397, 2020, doi: 10.1016/j.orcp.2020.07.007.

[7] R. Lu *et al.*, "Genomic characterisation and epidemiology of 2019 novel coronavirus: implications for virus origins and receptor binding," *Lancet*, vol. 395, no. 10224, pp. 565–574, 2020, doi: 10.1016/S0140-6736(20)30251-8.

[8] M. Y. Wang, R. Zhao, L. J. Gao, X. F. Gao, D. P. Wang, and J. M. Cao, "SARS-CoV-2: Structure, Biology, and Structure-Based Therapeutics Development," *Front. Cell. Infect. Microbiol.*, vol. 10, no. November, pp. 1–17, 2020, doi: 10.3389/fcimb.2020.587269.

[9] J. S. MacKenzie and D. W. Smith, "COVID-19: A novel zoonotic disease caused by a coronavirus from China: What we know and what we don't," *Microbiol. Aust.*, vol. 41, no. 1, pp. 45–50, 2020, doi: 10.1071/MA20013.

[10] A. E. Gorbalenya *et al.*, "The species Severe acute respiratory syndrome-related coronavirus: classifying 2019-nCoV and naming it SARS-CoV-2," *Nat. Microbiol.*, vol. 5, no. 4, pp. 536–544, 2020, doi: 10.1038/s41564-020-0695-z.

[11] K. Kousar, A. Majeed, F. Yasmin, W. Hussain, and N. Rasool, "Phytochemicals from Selective Plants Have Promising Potential against SARS-CoV-2: Investigation and Corroboration through Molecular Docking, MD Simulations, and Quantum Computations," *Biomed Res. Int.*, vol. 2020, 2020, doi: 10.1155/2020/6237160.

[12] C. Bai, Q. Zhong, and G. F. Gao, "Overview of SARS-CoV-2 genome-encoded proteins," vol. 65, no. 2, pp. 280–294, 2022.

[13] N. J. Hardenbrook and P. Zhang, "A structural view of the SARS-CoV-2 virus and its assembly," *Curr. Opin. Virol.*, vol. 52, pp. 123–134, 2022, doi: 10.1016/j.coviro.2021.11.011.

[14] Y. Huang, C. Yang, X. feng Xu, W. Xu, and S. wen Liu, "Structural and functional properties of SARS-CoV-2 spike protein: potential antivirus drug development for COVID-19," *Acta Pharmacol. Sin.*, vol. 41, no. 9, pp. 1141–1149, 2020, doi: 10.1038/s41401-020-0485-4.

[15] WHO EPI, "COVID-19 weekly epidemiological update," *World Heal. Organ.*, no. 58, pp. 1–23, 2021, [Online]. Available: https://www.who.int/publications/m/item/covid-19-weekly-epidemiological-update.

[16] M. Cascella, M. Rajnik, A. Cuomo, S. C. Dulebohn, and R. Di Napoli, "*Features, Evaluation and Treatment Coronavirus (COVID-19)".* [Updated 2022 May 4]

[17] Ministry of Health, "COVID-19 Weekly Epidemiological Update," *World Heal. Organ.*, no. February, pp. 1–33, 2021, [Online]. Available: https://www.who.int/publications/m/item/covid-19-weekly-epidemiological-update.

[18] D. Tian, Y. Sun, H. Xu, and Q. Ye, "The emergence and epidemic characteristics of the highly mutated SARS-CoV-2 Omicron variant," *J. Med. Virol.*, vol. 94, no. 6, pp. 2376–2383, 2022, doi: 10.1002/jmv.27643.

[19] W. T. Harvey *et al.*, "SARS-CoV-2 variants, spike mutations and immune escape," *Nat. Rev. Microbiol.*, vol. 19, no. 7, pp. 409–424, 2021, doi: 10.1038/s41579-021-00573-0.

[20] M. Hosseini, W. Chen, D. Xiao, and C. Wang, "Computational molecular docking and virtual screening revealed promising SARS-CoV-2 drugs," *Precis. Clin. Med.*, vol. 4, no. 1, pp. 1–16, 2021, doi: 10.1093/pcmedi/pbab001.

[21] B. A. Martinez-Guerra *et al.*, "Outcomes of patients with severe and critical COVID-19 treated with dexamethasone: a prospective cohort study," *Emerg. Microbes Infect.*, vol. 11, no. 1, pp. 50–59, 2022, doi: 10.1080/22221751.2021.2011619.

[22] S. Hong, H. Wang, Z. Zhang, and L. Qiao, "The roles of methylprednisolone treatment in patients with COVID-19: A systematic review and meta-analysis," *Steroids*, vol. 183, no. March, p. 109022, 2022, doi: 10.1016/j.steroids.2022.109022.

[23] C. S. Sharanya, A. Sabu, and M. Haridas, "Potent phytochemicals against COVID-19 infection from phyto-materials used as antivirals in complementary medicines: a review," *Futur. J. Pharm. Sci.*, vol. 7, no. 1, 2021, doi: 10.1186/s43094-021-00259-7.

[24] S. Cele *et al.*, "SARS-CoV-2 Omicron has extensive but incomplete escape of Pfizer BNT162b2 elicited neutralization and requires ACE2 for infection.," *medRxiv Prepr. Serv. Heal. Sci.*, 2021, doi: 10.1101/2021.12.08.21267417.

[25] A. Wilhelm *et al.*, "Reduced Neutralization of SARS-CoV-2 Omicron Variant by Vaccine Sera and monoclonal antibodies," *medRxiv*, p. 2021.12.07.21267432, 2021, [Online]. Available: https://www.medrxiv.org/content/10.1101/2021.12.07.21267432v2%0Ahttps://www.medrxiv.org/content/10.1101/2021.12.07.21267432v2.abstract.

[26] C. P. Kala, P. P. Dhyani, and B. S. Sajwan, "Developing the medicinal plants sector in northern India: Challenges and opportunities," *J. Ethnobiol. Ethnomed.*, vol. 2, no. August 2006, 2006, doi: 10.1186/1746-4269-2-32.

[27] A. Mansoori *et al.*, "Phytochemical Characterization and Assessment of Crude Extracts From Lantana camara L. for Antioxidant and Antimicrobial Activity," *Front. Agron.*, vol. 2, no. November, 2020, doi: 10.3389/fagro.2020.582268.

[28] S. S. Swain, S. K. Panda, and W. Luyten, "Phytochemicals against SARS-CoV as potential drug leads," *Biomed. J.*, vol. 44, no. 1, pp. 74–85, 2021, doi: 10.1016/j.bj.2020.12.002.

[29] A. Majeed, W. Hussain, F. Yasmin, A. Akhtar, and N. Rasool, "Virtual Screening of Phytochemicals by Targeting HR1 Domain of SARS-CoV-2 S Protein: Molecular Docking, Molecular Dynamics Simulations, and DFT Studies," *Biomed Res. Int.*, vol. 2021, 2021, doi: 10.1155/2021/6661191.

[30] D. Mannar *et al.*, "SARS-CoV-2 Omicron variant: Antibody evasion and cryo-EM structure of spike protein–ACE2 complex," *Science (80-.).*, vol. 375, no. 6582, pp. 760–764, 2022, doi: 10.1126/science.abn7760.

[31] E. F. Pettersen *et al.*, "UCSF Chimera - A visualization system for exploratory research and analysis," *J. Comput. Chem.*, 2004, doi: 10.1002/jcc.20084.

[32] N. Guex and M. C. Peitsch, "SWISS-MODEL and the Swiss-PdbViewer: An environment for comparative protein modeling," *Electrophoresis*, 1997, doi: 10.1002/elps.1150181505.

[33] N. M. O'Boyle, M. Banck, C. A. James, C. Morley, T. Vandermeersch, and G. R. Hutchison, "Open Babel," *J. Cheminform.*, vol. 3, no. 33, pp. 1–14, 2011, [Online]. Available: https://jcheminf.biomedcentral.com/track/pdf/10.1186/1758-2946-3-33.

[34] C. Shi, F. Wu, X. Zhu, and J. Xu, "Incorporation of β-sitosterol into the membrane increases resistance to oxidative stress and lipid peroxidation via estrogen receptor-mediated PI3K/GSK3β signaling," *Biochim. Biophys. Acta - Gen. Subj.*, vol. 1830, no. 3, pp. 2538–2544, 2013, doi: 10.1016/j.bbagen.2012.12.012.

[35] A. Singh, "Sitosterol as an antioxidant in frying oils," *Food Chem.*, vol. 137, no. 1–4, pp. 62–67, 2013, doi: 10.1016/j.foodchem.2012.10.008.

[36] R. Liz *et al.*, "Acute effect of β-sitosterol on calcium uptake mediates anti-inflammatory effect in murine activated neutrophils," *J. Pharm. Pharmacol.*, vol. 65, no. 1, pp. 115–122, 2013, doi: 10.1111/j.2042-7158.2012.01568.x.

[37] M. Sankar *et al.*, "In silico Screening of Natural Phytocompounds Towards Identification of Potential Lead Compounds to Treat COVID-19," *Front. Mol. Biosci.*, vol. 8, no. July, 2021, doi: 10.3389/fmolb.2021.637122.

[38] Y. Kashiwada, F. Hashimoto, L. M. Cosentino, C. H. Chen, P. E. Garrett, and K. H. Lee -, "Betulinic acid and dihydrobetulinic acid derivatives as potent anti-HIV agents," *J. Med. Chem.*, vol. 39, no. 5, pp. 1016–1017, 1996, doi: 10.1021/jm950922q.

[39] M. S. De Sá *et al.*, "Antimalarial activity of betulinic acid and derivatives in vitro against Plasmodium falciparum and in vivo in P. berghei-infected mice," *Parasitol. Res.*, vol. 105, no. 1, pp. 275–279, 2009, doi: 10.1007/s00436-009-1394-0.

[40] J. Zhao *et al.*, "Antitumor activity of betulinic acid and betulin in canine cancer cell lines," *In Vivo (Brooklyn).*, vol. 32, no. 5, pp. 1081–1088, 2018, doi: 10.21873/invivo.11349.

[41] G. A. Kurian, S. Suryanarayanan, A. Raman, and J. Padikkala, "Antioxidant effects of ethyl acetate extract of Desmodium gangeticum root on myocardial ischemia reperfusion injury in rat hearts," *Chin. Med.*, vol. 5, pp. 1–7, 2010, doi: 10.1186/1749-8546-5-3.

[42] M. Obulesu and D. M. Rao, "Effect of plant extracts on Alzheimer's disease: An insight into therapeutic avenues," *J. Neurosci. Rural Pract.*, vol. 2, no. 1, pp. 56–61, 2011, doi: 10.4103/0976-3147.80102.

[43] R. M. Ogboye, R. B. Patil, S. O. Famuyiwa, and K. O. Faloye, "Novel α-amylase and α-glucosidase inhibitors from selected Nigerian antidiabetic plants: an in silico approach," *J. Biomol. Struct. Dyn.*, vol. 0, no. 0, pp. 1–10, 2021, doi: 10.1080/07391102.2021.1883480.

[44] H. Li *et al.*, "Glycyrrhetinic acid: A potential drug for the treatment of COVID-19 cytokine storm," *Phytomedicine*, vol. 102, no. January, p. 154153, 2022, doi: 10.1016/j.phymed.2022.154153.

[45] G. Renda, İ. Gökkaya, and D. Şöhretoğlu,

"Immunomodulatory properties of triterpenes," *Phytochem. Rev.*, vol. 21, no. 2, pp. 537–563, 2022, doi: 10.1007/s11101-021-09785-x.

[46] D. Dastan, P. Salehi, A. Reza Gohari, S. N. Ebrahimi, A. Aliahmadi, and M. Hamburger, "Bioactive Sesquiterpene Coumarins from Ferula pseudalliacea," *Planta Med.*, vol. 80, no. 13, pp. 1118–1123, 2014, doi: 10.1055/s-0034-1382996.

[47] M. S. Kim, K. S. Oh, J. H. Lee, S. Y. Ryu, J. Mun, and B. H. Lee, "Kamolonol suppresses angiotensin II-induced stress fiber formation and cellular hypertrophy through inhibition of Rho-associated kinase 2 activity," *Biochem. Biophys. Res. Commun.*, vol. 438, no. 2, pp. 318–323, 2013, doi: 10.1016/j.bbrc.2013.07.069.

[48] O. K. Popoola, A. M. Elbagory, F. Ameer, and A. A. Hussein, "Marrubiin," *Molecules*, vol. 18, no. 8, pp. 9049–9060, 2013, doi: 10.3390/molecules18089049.

[49] L. Huang *et al.*, "Anti-inflammatory effects of maslinic acid, a natural triterpene, in cultured cortical astrocytes via suppression of nuclear factor-kappa B," *Eur. J. Pharmacol.*, vol. 672, no. 1–3, pp. 169–174, 2011, doi: 10.1016/j.ejphar.2011.09.175.

[50] F. J. Reyes-Zurita, G. Pachón-Peña, D. Lizárraga, E. E. Rufino-Palomares, M. Cascante, and J. A. Lupiáñez, "The natural triterpene maslinic acid induces apoptosis in HT29 colon cancer cells by a JNK-p53-dependent mechanism," *BMC Cancer*, vol. 11, 2011, doi: 10.1186/1471-2407-11-154.

[51] G. Lozano-Mena, M. Sánchez-González, M. E. Juan, and J. M. Planas, "Maslinic acid, a natural phytoalexin-type triterpene from olives - A promising nutraceutical?," *Molecules*, vol. 19, no. 8, pp. 11538–11559, 2014, doi: 10.3390/molecules190811538.

[52] A. Hussain Shaik, S. N. Rasool, M. A. Kareem, G. S. Krushna, P. M. Akhtar, and K. L. Devi, "Maslinic acid protects against isoproterenol-induced cardiotoxicity in albino Wistar rats," *J. Med. Food*, vol. 15, no. 8, pp. 741–746, 2012, doi: 10.1089/jmf.2012.2191.

[53] T. Guan *et al.*, "Maslinic acid, a natural inhibitor of glycogen phosphorylase, reduces cerebral ischemic injury in hyperglycemic rats by GLT-1 up-regulation," *J. Neurosci. Res.*, vol. 89, no. 11, pp. 1829–1839, 2011, doi: 10.1002/jnr.22671.

[54] A. Sen, "Prophylactic and therapeutic roles of oleanolic acid and its derivatives in several diseases," *World J. Clin. Cases*, vol. 8, no. 10, pp. 1767–1792, 2020, doi: 10.12998/wjcc.v8.i10.1767.

[55] N. A. Luchnikova, V. V Grishko, and I. B. Ivshina, "Biotransformation of Oleanane and Ursane Triterpenic Acids," *Molecules*, vol. 25, no. 23: 5526, 2020, doi: 10.3390/molecules25235526.

[56] S. C. Bachar, K. Mazumder, R. Bachar, and A. Aktar, "A Review of Medicinal Plants with Antiviral Activity Available in Bangladesh and Mechanistic Insight Into Their Bioactive Metabolites on," vol. 12, no. November, pp. 1–20, 2021, doi: 10.3389/fphar.2021.732891.

[57] Sultana, Tahira, Mohammad K. Okla, Madiha Ahmed, Nosheen Akhtar, Abdulrahman Al-Hashimi, Hamada Abdelgawad, and Ihsan-ul-Haq. 2021. D. "Withaferin A : From Ancient Remedy to Potential Drug Candidate", *Molecules*, vol. 26, no. 24: 7696. doi: 10.3390/molecules26247696.

[58] V. Kumar *et al.*, "Withanone and Withaferin-A are predicted to interact with transmembrane protease serine 2 (TMPRSS2) and block entry of SARS-CoV-2 into cells," *J. Biomol. Struct. Dyn.*, vol. 40, no. 1, pp. 1–13, 2022, doi: 10.1080/07391102.2020.1775704.

[59] V. P. Wadegaonkar and P. A. Wadegaonkar, "Withanone as an inhibitor of survivin : A potential drug candidate for cancer therapy," *J. Biotechnol.*, vol. 168, no. 2, pp. 229–233, 2013, doi: 10.1016/j.jbiotec.2013.08.028.

[60] N. J. Dar, J. A. Bhat, N. K. Satti, P. R. Sharma, A. Hamid, and M. Ahmad, "Withanone , an Active Constituent from Withania somnifera , Affords Protection Against NMDA-Induced Excitotoxicity in Neuron-Like Cells," *Mol. Neurobiol.*, 2016, doi: 10.1007/s12035-016-0044-7.

[61] J. Kaur *et al.*, "International Journal of Biological Macromolecules Molecular mechanism of anti-SARS-CoV2 activity of Ashwagandha-derived withanolides," *Int. J. Biol. Macromol.*, vol. 184, no. December 2020, pp. 297–312, 2021, doi: 10.1016/j.ijbiomac.2021.06.015.

[62] P. T. White, C. Subramanian, H. F. Motiwala, and M. S. Cohen, *Natural Withanolides in the Treatment of Chronic Diseases*. 2016.

[63] J. Gu *et al.*, "Cytotoxic and Antimicrobial Constituents of the Bark of Diospyros maritima Collected in Two Geographical Locations in Indonesia," vol. 1, pp. 1156–1161, 2004.

[64] J. T. Ortega, B. Jastrzebska, and H. R. Rangel, "Omicron SARS-CoV-2 Variant Spike Protein Shows an Increased Affinity to the Human ACE2 Receptor: An In Silico Analysis," *Pathogens*, vol. 11, no. 1, 2022, doi: 10.3390/pathogens11010045.

[65] S. Kumar, T. S. Thambiraja, K. Karuppanan, and G. Subramaniam, "Omicron and Delta variant of SARS-CoV-2: A comparative computational study of spike protein," *J. Med. Virol.*, vol. 94, no. 4, pp. 1641–1649, 2022, doi: 10.1002/jmv.27526.

[66] Morris, G. M., Huey, R., Lindstrom, W., Sanner, M. F., Belew, R. K., Goodsell, D. S., & Olson, A. J. (2009). AutoDock4 and AutoDockTools4: Automated docking with selective receptor flexibility. *Journal of Computational Chemistry*, *30*(16), 2785–2791.

[67] R.A. Laskowski and M.B. Swindells, -LigPlot+: Multiple ligand-protein interaction diagrams for dru discovery, *J. Chem. Inf. Model.*, 2011, doi: 10.1021/ci200227u.

[68] B. Jayaram, T. Singh, G. Mukherjee, A. Mathur, S. Shekhar, and V. Shekhar, ―Sanjeevini: a freely accessible web-server for target directed lead molecule discovery, *BMC Bioinformatics*, 2012, doi: 10.1186/1471-2105-13-S17-S7.

[69] C. A. Lipinski, ―Lead- and drug-like compounds: The rule-of-five revolution, *Drug Discovery Today: Technologies*. 2004, doi: 10.1016/j.ddtec.2004.11.007.

[70] A. C. Pushkaran, P. Nath EN, A. R. Melge, R. Puthiyedath, and C. G. Mohan, "A phytochemical-based medication

search for the SARS-CoV-2 infection by molecular docking models towards spike glycoproteins and main proteases," *RSC Adv.*, vol. 11, no. 20, pp. 12003–12014, 2021, doi: 10.1039/d0ra10458b.

[71] C. A. Lipinski, F. Lombardo, B. W. Dominy, and P. J. Feeney, "Experimental and computational approaches to estimate solubility and permeability in drug discovery and development settings," *Adv. Drug Deliv. Rev.*, vol. 23, no. 1–3, pp. 3–25, 1997, doi: 10.1016/S0169-409X(96)00423-1.